

Scientific paper

Serviceability Performance Evaluation of RC Flexural Members Improved by Using Low-Shrinkage High-Strength Concrete

Makoto Tanimura¹, Ryoichi Sato² and Yoichi Hiramatsu³

Received 16 February 2007, accepted 21 April 2007

Abstract

This paper aims to show the importance of autogenous shrinkage for the serviceability performance of reinforced high-strength concrete (HSC) flexural beams, and also the effectiveness of low-shrinkage HSCs (LS-HSC) made by using expansive additive and/or shrinkage-reducing chemical agent and/or Belite-rich low-heat Portland cement for improving the flexural serviceability performance of beam. From the design equation point of view, this paper also proposes a new concept for evaluating flexural crack width and deformation of RC beams taking into consideration the early age deformation of concrete before loading. The experimental results show that autogenous shrinkage of HSC significantly affects increases in crack width and deformation of RC beams, while LS-HSCs markedly improves their serviceability performance. The present concept, which takes into account strain change in tension reinforcement and curvature change in the cracked section before and after loading, is effective in explaining the effects of shrinkage and expansion of concrete before loading on maximum crack width and flexural deformation of RC beams. JSCE (Japan Society of Civil Engineers) code equations for predicting maximum crack width and flexural deformation into which the present concept is incorporated improve the prediction accuracy compared with conventional equations and show fairly good agreement with experimental results.

1. Introduction

The development of superplasticizer and the widespread use of supplementary fine mineral powders such as silica fume and granulated blast-furnace slag have enabled the production of high-strength and/or high-flowability concrete. High-strength concrete (HSC) has been widely studied over the last decade and has been increasingly applied to enhance the durability and structural performance of concrete structures. However, such low water-to-binder ratio concretes are known to shrink significantly at early ages, which is likely to be caused by autogenous (self-desiccation) shrinkage, and frequently exhibit increased sensitivity to early-age cracking (Pailere *et al.* 1989, Tazawa *et al.* 1992a, Schrage *et al.* 1992, Tazawa *et al.* 1994). Control of cracking in RC members is always a matter of concern because the durability of concrete structures declines with crack formation. HSC is expected to yield more durable structural members, and therefore more severe control of cracking for HSC, compared to conventional concrete, is essential. Thus, the establishment of a technique for minimizing autogenous shrinkage in HSC is an important task.

Recently, experimental investigations on how to con-

trol autogenous shrinkage have been carried out comprehensively from a material point of view (JCI 1999). These studies revealed that expansive additive (Tazawa *et al.* 1992b, Hori *et al.* 1998, Tanimura *et al.* 2000, Schwartzentruber *et al.* 2002), shrinkage-reducing chemical agent (Tazawa *et al.* 1992b, Takeuchi *et al.* 1997, Tanimura *et al.* 2000, Weiss *et al.* 1999, Holt *et al.* 2000, Bentz *et al.* 2001, Berke *et al.* 2003), as well as Portland cement containing higher C₂S content and lower C₃A content are obviously effective in reducing autogenous shrinkage (Tazawa *et al.* 1995, Takeuchi *et al.* 1997, Hori *et al.* 1998, Tanimura *et al.* 2000). Additionally, the effect of the combination of the above-mentioned materials on reducing autogenous shrinkage has been investigated, and HSCs with lower risk of early-age cracking have been developed (Ogawa *et al.* 1995, Chikamatsu *et al.* 1997, Sato *et al.* 1999, Tanimura *et al.* 2000, Kameta *et al.* 2000, Hori *et al.* 2001, Tanimura *et al.* 2001a, Tanimura *et al.* 2002a). Very recently, techniques referred to as internal water curing of concrete that enable counteracting of self-desiccation by partially replacing normal weight aggregate with pre-saturated lightweight aggregate or adding super-adsorbent polymer particles as concrete admixture, have been reported (Bentur *et al.* 2001, Jensen *et al.* 2001, Jensen *et al.* 2002).

However, studies on the effect of autogenous shrinkage and the effectiveness of low-shrinkage HSC from the viewpoint of structural performance of RC members have been insufficient. Further, there are only a few reports on methods for evaluating the serviceability performance of RC members considering the effect of autogenous shrinkage/expansion before loading (Tani-

¹Research Scientist, Research & Development Center, Taiheiyo Cement Corporation, Japan.

E-mail: makoto_tanimura@taiheiyo-cement.co.jp

²Professor, Department of Social and Environmental Engineering, Hiroshima University, Japan.

³PC Construction Division, P.S. Mitsubishi Construction Co., Ltd., Japan.

mura *et al.* 2001b, Tanimura *et al.* 2002b, Sato *et al.* 2003), even though such evaluation is required for service life prediction.

In light of the above situation, the present paper aims to show the importance of autogenous shrinkage for the serviceability performance of reinforced W/C = 0.3 high-strength concrete (HSC) flexural beams, and also the effectiveness of low-shrinkage HSCs made by using expansive additive and/or shrinkage-reducing chemical agent and/or Belite-rich low-heat Portland cement for improving the flexural serviceability performance of beams. From the design equation point of view, this paper also investigates and proposes a general method for evaluating maximum crack width and deformation of RC flexural beams, considering the early age deformation of concrete before loading.

2. Experimental program

2.1 Materials

The materials used in the study are listed in **Table 1**. The contents of C₃S, C₂S, C₃A and C₄AF of ordinary Portland cement (OPC), calculated using Bogue's equations, were 52%, 24%, 9%, and 9%, respectively. On the other hand, those of Belite-rich low-heat Portland cement (LPC) were 26%, 55%, 3%, and 9%, respectively. A previous study revealed that the mineral composition of cement affects autogenous shrinkage significantly (Tazawa *et al.* 1993, Tazawa *et al.* 1997). Based on Eq. 1 below, derived by Miyazawa & Tazawa (Miyazawa *et al.* 1996), LPC-based mixtures can be predicted to have less autogenous shrinkage.

$$\varepsilon_{p\infty} = 2.15 \cdot (C_3S\%) - 5.49 \cdot (C_2S\%) + 68.7 \cdot (C_3A\%) + 48.5 \cdot (C_4AF\%) \quad (1)$$

where, $\varepsilon_{p\infty}$ is the ultimate value of autogenous shrinkage strain (original length: 24 hours after casting) of cement paste with W/C = 0.3 ($\times 10^{-6}$), and (C₃S%), (C₂S%), (C₃A%), and (C₄AF%) are the %mass

content of C₃S, C₂S, C₃A, and C₄AF, respectively.

2.2 Mixture proportions

Ten HSCs with fixed water-to-binder ratios of 0.3 were prepared in order to investigate the effect of autogenous shrinkage/expansion on the serviceability performance of RC flexural beams. **Table 2** lists the mix proportions of these concretes as well as their respective slump flow value, air content, and temperature measured just before the concrete was placed. The replacement dosages of EX and SRA were set to 30 kg/m³ and 6 kg/m³, respectively, regardless of the type of cement. The concrete quality, referred to as NC1 and NC2, represents a reference HSC made using OPC. NE1, NS, and NE1S denote LS-HSC made using OPC with EX1, SRA, and EX1 and SRA, respectively. LC denotes LS-HSC with LPC, and LE1, LS, and LE1S correspond to concretes consisting of LPC with EX1, SRA, and EX1 and SRA, respectively.

2.3 Specimens

The RC beam specimens for investigating the shrinkage/expansion-restrained stress, cracking behaviors, and deflections are shown in **Fig. 1**. Self-temperature compensated wire strain gauges were attached to the upper and bottom sides of the tension reinforcement at mid-span in order to measure the reinforcement strain until loading of the beam. One specimen was prepared for each mixture.

Prismatic specimens with the same cross section as that of the RC beams were prepared to measure free deformation, as shown in **Fig. 2**. One specimen was prepared for each of NC1, NE1, NS, NE, LC, LE1, LS, and LE1S, and eight specimens were prepared for each of NC2 and NE2S.

To minimize the friction between the mold and the concrete specimen, a 1.0 mm thick Teflon sheet was placed at the bottom of the mold. Further, a 3 mm thick polystyrene board was placed on both ends of the mold. All the surfaces of the beam specimen mold were covered with a 0.1 mm thick polyester film.

Table 1 Materials.

Material	Symbol	Type / Characteristics
Cement	OPC	Ordinary Portland cement / density: 3.16 g/cm ³ , SSA: 3310 cm ² /g
	LPC	Low-heat Portland cement / density: 3.22 g/cm ³ , SSA: 3280 cm ² /g
Expansive additive	EX1	Calcium-sulfoaluminate based / density: 2.96 g/cm ³ , SSA: 3050 cm ² /g
	EX2	Lime-based / density: 3.14 g/cm ³ , SSA: 3310 cm ² /g
Shrinkage reducer	SRA	Lower-alcohol alkyleneoxide adduct / density: 1.00 g/cm ³
Fine aggregate	S	Pit sand / density: 2.62 g/cm ³ , absorption: 1.66%, F.M.: 2.84
Coarse aggregate	G	Crushed sand stone / maximum size: 20 mm, density: 2.64 g/cm ³ , absorption: 0.85%, F.M.: 6.61
Water reducer	SP	Polycarboxylic acid based high-range water reducer / density: 1.05 g/cm ³

SSA: Specific surface area measured by Blaine's Method, F.M.: Fineness modulus

Table 2 Mix proportions and fresh properties of concrete.

Mix proportions and fresh properties	Symbol of concrete									
	NC1	NE1	NS	NE1S	LC	LE1	LS	LE1S	NC2	NE2S
Type of cement	OPC				LPC				OPC	
W/(C+EX)	0.3									
W* (kg/m ³)	175		169		175		169		175	169
C (kg/m ³)	583	543	583	543	583	543	583	543	583	543
EX (kg/m ³)	-	40	-	40	-	40	-	40	-	40
SRA (kg/m ³)	-	-	6	6	-	-	6	6	-	6
S (kg/m ³)	800	798	800	798	809	806	809	806	800	798
G (kg/m ³)	832									
SP (kg/m ³)	5.25	5.42	5.83	6.70	2.92	3.38	2.97	3.50	4.08	3.50
Slump flow (mm)	623	423	630	625	520	570	530	635	550	475
Air content (%)	1.0	0.6	1.5	1.3	2.1	1.3	1.2	1.4	2.9	1.6
Temperature (°C)	19.9	21.2	18.0	19.0	18.2	17.0	18.2	17.6	14.3	15.3

(*) The unit water content includes SP.

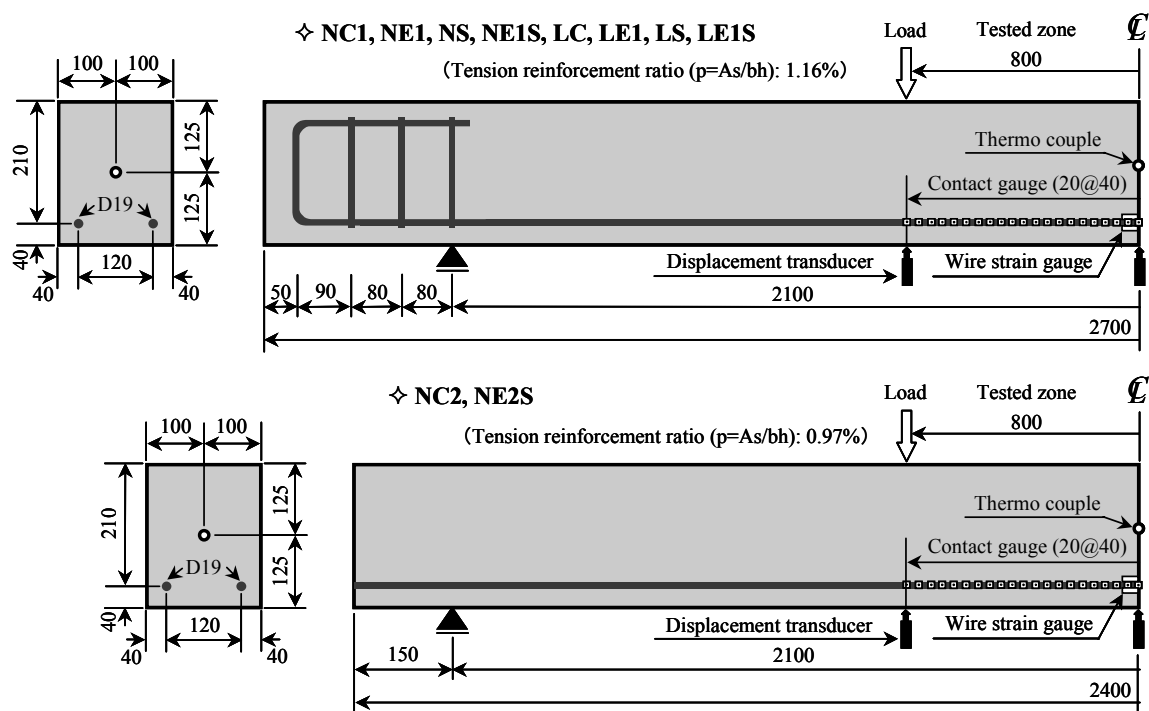


Fig. 1 Dimensions and configuration of RC beam specimens (unit: mm).

In addition, three cylindrical specimens of 100 x 200 mm for each mixture were prepared to measure the compressive strength and Young's modulus. Three cylindrical specimens measuring 150 x 200 mm were also prepared for each mixture in order to measure the splitting tensile strength.

After demolding, all the specimens were promptly sealed with a 0.05 mm thick aluminum adhesive tape to prevent water evaporation. The demolding time of the OPC-based and LPC-based mixtures were one day and

two days after casting, respectively. The specimens were cured at room temperature.

2.4 Loading and measurements

Two-point loading (4-point bending) was accurately applied to the RC beams. The span and pure moment zone of the beams were 2100 mm and 800 mm. Crack widths at the depth of tension reinforcement were measured using a contact-type strain gauge with a minimum graduation of 0.001 mm. To measure the crack

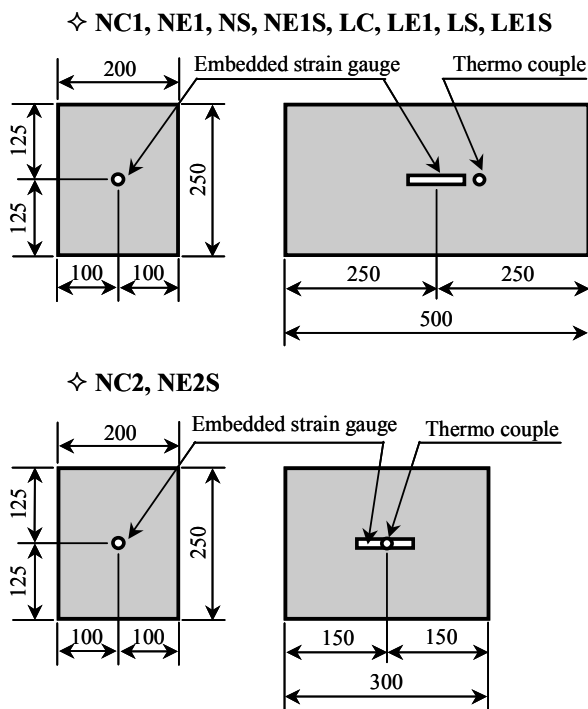


Fig. 2 Specimens used in free deformation (unit: mm).

width as accurately as possible, a distance of 20 mm between each contact point was adopted. Deflections were measured by using displacement transducers with a minimum graduation of 0.001 mm. The deflection measurement results were used to calculate the average curvature in the pure moment zone.

In order to measure the free deformation, an embedded strain gauge with a reference length of 100 mm and low elastic modulus of 39 N/mm², and a thermocouple were placed at the center of the specimens. The NC1, NE1, NS, NE1S, LC, LE1, LS, and LE1S specimens were kept sealed with aluminum adhesive tape for approx. one year to evaluate the autogenous shrinkage/expansion strain. On the other hand, four specimens for NC2 and NE2S were kept sealed with aluminum adhesive tape for two years to evaluate the autogenous shrinkage/expansion strain, while the other four specimens were stripped from the aluminum adhesive tape at the age of 30 days to evaluate the total shrinkage/expansion strain under a drying condition. The expansion/shrinkage strain of

concrete was determined by subtracting the thermal strain from the measured strain, assuming the coefficient of thermal expansion of concrete to be $10 \times 10^{-6}/^{\circ}\text{C}$. Measurement began immediately after the concrete was placed.

The compressive strength, Young's modulus, and the splitting tensile strength of concrete were measured in accordance with JIS A 1108, JIS A 1149, and JIS A 1113, respectively.

3. Experimental results

3.1 Mechanical properties of concrete

Table 3 tabulates the compressive strength, splitting tensile strength, and Young's modulus of the tested sealed plain concretes. The compressive strengths and splitting tensile strengths of the investigated mixtures ranged from 70.8 to 91.4 N/mm², and from 4.10 to 5.77 N/mm², respectively. Therefore, the water/binder ratio for achieving the required strength should be varied by the addition of EX and/or SRA as well as the type of cement.

3.2 Shrinkage/expansion strain of concrete

The experimental results on autogenous shrinkage/expansion strains for all the investigated mixtures are shown in Fig. 3. The data are plotted as a function of temperature-adjusted concrete age calculated by Eq. 2 below (CEB 1990) from the viewpoint of the hydration process:

$$t = \sum_{i=1}^n \Delta t_i \exp \left[13.65 - \frac{4000}{273 + T(\Delta t_i) / T_0} \right] \quad (2)$$

where, t = temperature adjusted concrete age, Δt_i = number of days when a temperature T ($^{\circ}\text{C}$) prevails, and $T_0 = 1^{\circ}\text{C}$.

The reference NC1/NC2 mixtures showed a significant autogenous shrinkage strain of approx. 300×10^{-6} and approx. 500×10^{-6} at the age of 28 days and one year, respectively. OPC-based HSCs containing expansive additive and/or shrinkage-reducing agent showed a smaller autogenous shrinkage than that of NC1/NC2. The autogenous shrinkage observed for LC was markedly small compared with that observed for NC, almost

Table 3 Mechanical properties of sealed plain concretes just before loading of RC beams.

Symbol	NC1	NE1	NS	NE1S	LC	LE1	LS	LE1S	NC2	NE2S
Age (days)	63	65	57	70	70	64	64	61	30	30
Compressive strength (N/mm ²)	79.1	70.8	91.4	90.2	73.9	79.6	74.4	75.5	80.5	70.8
Young's modulus (kN/mm ²)	37.3	36.7	40.4	38.4	38.8	38.9	38.1	36.7	37.7	38.7
Splitting tensile strength (N/mm ²)	4.77	5.07	5.47	5.77	4.58	4.50	4.16	4.10	4.15	4.14

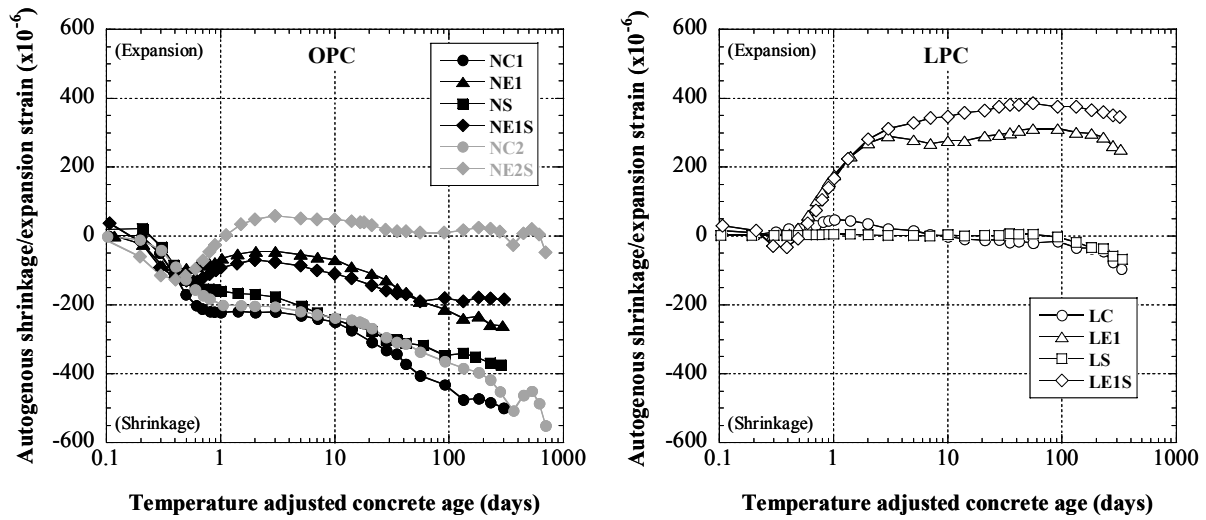


Fig. 3 Autogenous shrinkage/expansion strain of concrete.

Table 4 Autogenous strain and restrained stress at extreme bottom fiber just before loading.

Symbol	NC	NE1	NS	NE1S	LC	LE1	LS	LE1S	NC2	NE2S
Loading age (days)	63	65	57	70	70	64	64	61	32	32
Autogenous strain ($\times 10^{-6}$)	-397	-174	-313	-175	-12	311	5	383	-259	29
Restrained stress (N/mm^2)	1.27	0.11	1.00	-0.03	0.16	-1.45	-0.06	-1.52	0.80	-0.49

zero until the age of 100 days. LPC-based concretes that use expansive additive (LE1 and LE1S) showed expansion rather than shrinkage even though there was no difference in unit content of expansive additive between the OPC-based and the LPC-based concretes. A synergistic effect of using both expansive additive and shrinkage-reducing agents was observed for the concrete with LPC cement; i.e., the compensation quantity in the strain of LE1S, which is 395×10^{-6} , was greater than the summation of those of LE1 and LS corresponding to 323×10^{-6} and 17×10^{-6} , respectively, as shown in **Table 4**.

In addition, the drying shrinkage strain of NE2S, which is determined by subtracting the autogenous shrinkage strain from the total shrinkage strain, was approx. 50% of that of NC2 at the age of two years, as shown in **Fig. 4**. As a result, the total shrinkage of NE2S is markedly smaller than that of NC2; the former was approx. 15% of that of the latter at the age of two years. Thus, the combination of an expansive additive and a shrinkage-reducing chemical agent is effective for reducing shrinkage from early-ages to long-term ages.

3.3 Restrained-shrinkage/expansion stress

Figure 5 shows the restrained stress histories in concrete at the extreme bottom fiber due to the restraint of rein-

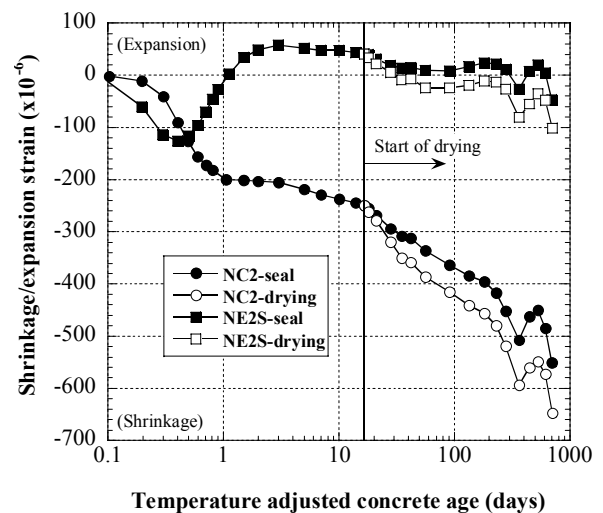


Fig. 4 Autogenous shrinkage/expansion strain of concrete.

forcements, determined by Eq. 3. This equation is derived from the equilibrium of the force among concrete and reinforcement as well as Navier's assumption, in which the stress is positive in tension and negative in compression.

$$P_s = A_s \cdot E_s \cdot \varepsilon_s$$

$$\sigma_c = -\frac{P_s}{A_c} \left[1 + \frac{(d - C_g)(h - C_g)}{I_c / A_c} \right] \quad (3)$$

where, P_s = axial force in reinforcement, E_s = Young's modulus of reinforcement, ε_s = measured strain in reinforcement, A_s = cross-sectional area of reinforcement, σ_c = stress at the extreme bottom fiber, I_c = moment of inertia of gross concrete section, A_c = cross-sectional area of concrete, d = effective depth, h = height of beam, and C_g = distance from the extreme upper fiber to the centroid of the gross concrete section.

The restrained stress just before loading is listed in Table 4.

NC1 showed the highest tensile stress, approx. 1.3 N/mm². On the other hand, the tensile stresses of NE1, NE1S, LC, and LS were controlled to be negligible compared with those of NC1/NC2. LE1 and LE1S showed restrained stress in compression of approx. 1.5 N/mm². Thus, using Belite-rich low-heat Portland cement, expansive additive, shrinkage reducing agent, or a combination of these is effective for compensating autogenous shrinkage and resultant induced stresses.

4. Serviceability performance of RC beams

4.1 Flexural cracking moment

Figure 6 shows the flexural cracking moments (M_{cr}), determined from the bending moment for a case where the deflection was drastically changed. The M_{cr} , calculated by using the measured splitting tensile strength and either neglecting or considering the restrained stress at the extreme bottom fiber, is shown in the same figure. The measured M_{cr} of the NC1-RC beam is reduced to approx. 60% of that of the calculated M_{cr} . On the other hand, the measured M_{cr} values of NE1-, NE1S-, NE2S-,

LC-, and LS-RC beams are approximately 1.3 to 2 times higher than the M_{cr} of the NC1/NC2-RC beam, indicating a marked increase in M_{cr} caused by reducing autogenous shrinkage. This effect is observed even though the difference in M_{cr} s calculated by neglecting the restrained stress is considered. In the case of LE1- and LE1S-RC beams with the compressive stress located at the extreme bottom fiber, the measured M_{cr} increases to approx. 2.5 times of that of the NC1-RC beam. Regarding the evaluation of M_{cr} , the M_{cr} calculated by considering the restrained stress obviously gives closer results to the measured values than evaluation in which the restrained stress is neglected.

4.2 Crack width

Figure 7 shows the ratio of maximum crack width or maximum crack spacing of LS-HSC RC beams, measured when the stress in tension reinforcement calculated in accordance with conventional RC theory was 200N/mm². The maximum crack widths of low-shrinkage HSC-RC beams are reduced to approx. 20-40% of those of the NC-RC beam, while the maximum crack spacings of the former are increased to approximately 10-40% of those of the latter. Thus wider crack spacing resulted in a smaller crack width, a result that differs from the conventional concept. These findings indicate that low-shrinkage HSCs are clearly effective for improving cracking behavior that has declined due to autogenous shrinkage.

4.3 Curvature

Figure 8 shows the ratio of average curvature of LS-HSC RC beams, measured when the stress in tension reinforcement calculated in accordance with conventional RC theory was 200N/mm². The average curvature calculated by the JSCE design code (JSCE 2002) is shown in the same figure. The measured average

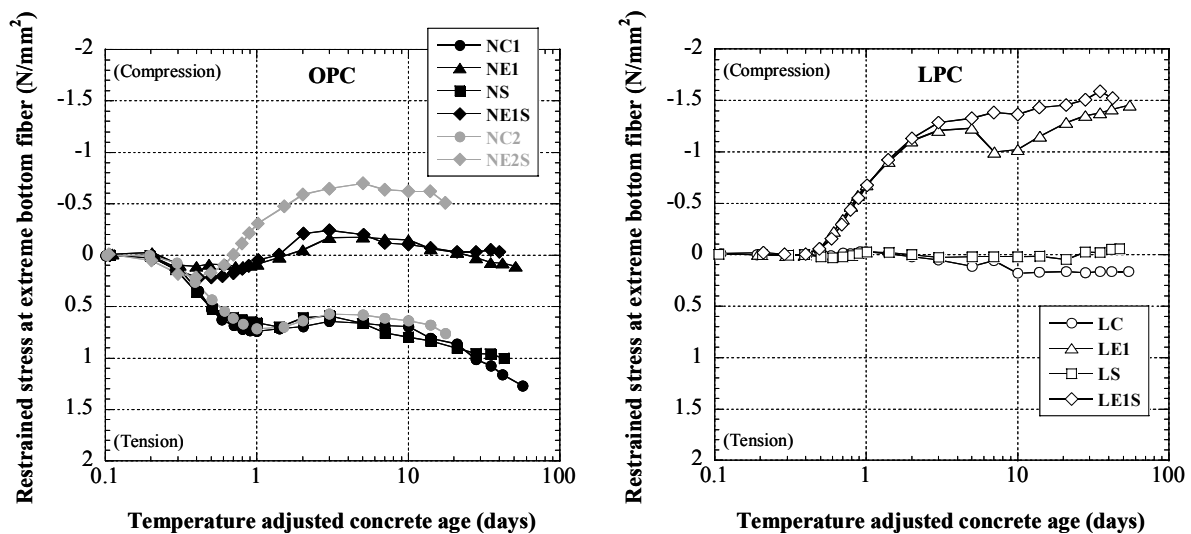


Fig. 5 Restrained stress in concrete at extreme bottom fiber.

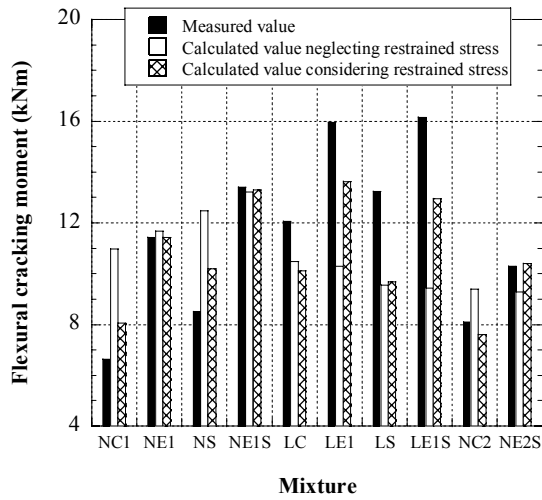


Fig. 6 Flexural cracking moment.

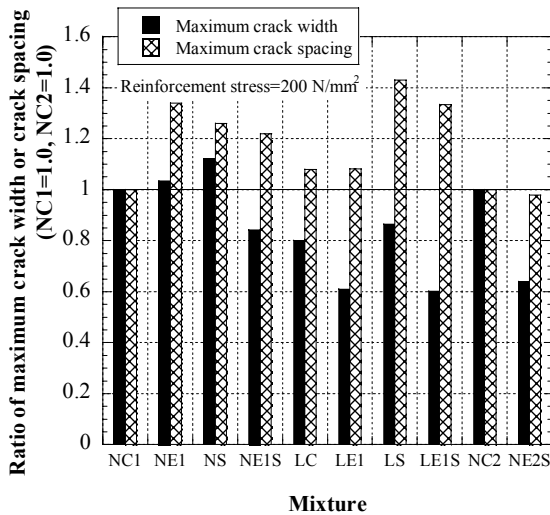


Fig. 7 Comparison of maximum crack width and maximum crack spacing.

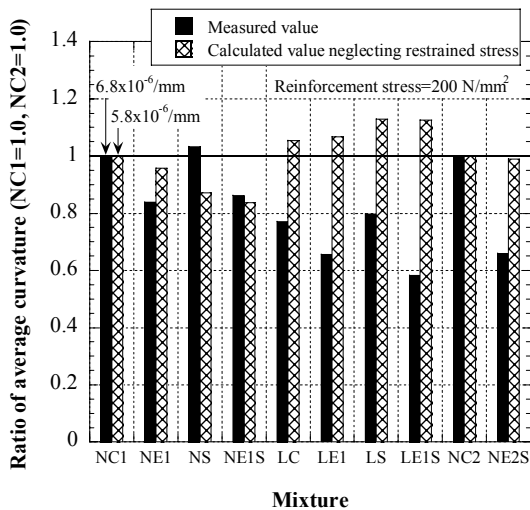


Fig. 8 Comparison of average curvature.

curvature of the NC1-RC beam is increased to approx. 20% of that of the calculated average curvature, while the measured average curvatures of low-shrinkage HSC-RC beams are approx. 15-40% smaller than that of the NC1/NC2-RC beam. LPC-based mixtures are particularly effective in reducing curvature when considering the larger calculated curvature.

5. A new concept for evaluating the serviceability performance of RC flexural members

5.1 Maximum crack width

Figure 9 shows the relationship between maximum crack width and stress in tension reinforcement calculated in accordance with conventional RC theory, neglecting the early age deformation of concrete (autogenous shrinkage/expansion) on crack width. The maximum crack widths calculated by using conventional reinforcement stress are also shown in the same figure. The data in the figure shows significant differences in crack width among the mixtures. The greater the shrinkage/expansion of the concrete, the wider/smaller the maximum crack width measured in RC beams. The significant difference in crack width among mixtures can be explained by the fact that the strain change in tension reinforcement varies by the shrinkage/expansion of the concrete before loading. That is, when concrete shrinks or expands in reinforced concrete, tensile or compressive stress is induced in the concrete, and an equal and opposite stress is simultaneously induced in the reinforcements. On the other hand, the effect of early age deformation on the magnitude of strain in reinforcements at a cracked section should be negligible based on the equilibrium requirement after load induced cracks develop in concrete members. Therefore, the change in strain in reinforcements before and after loading should be dif-

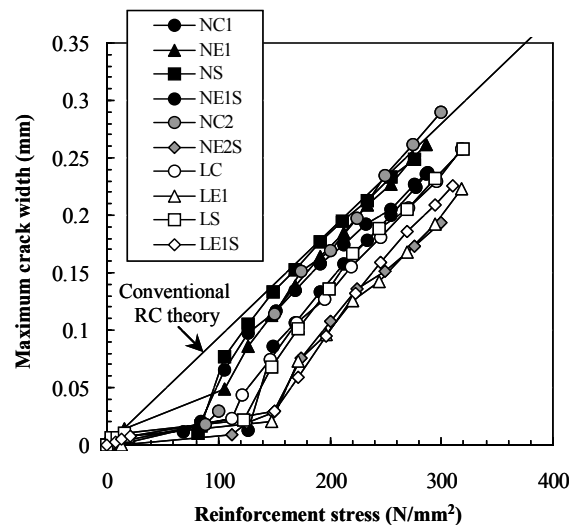


Fig. 9 Maximum crack width versus reinforcement stress based on conventional RC theory.

ferent among beams made of high-shrinkage HSC and low-shrinkage HSC.

Figure 10 shows the basic concept of the change in strain in longitudinal reinforcements from the state where the stress in concrete at the depth of the tension reinforcements is zero (zero stress condition). In this figure, $M_{cr,ex}$, $M_{cr,non}$, and $M_{cr,sh}$ denote cracking moments of beams made of expansive concrete, concrete with no shrinkage, and shrinking concrete, respectively. Furthermore, $\epsilon_{s,ex}$, $\epsilon_{s,sh}$ and $\epsilon_{s0,ex}$, $\epsilon_{s0,sh}$, and $\epsilon_{s,load}$ denote strains in tension reinforcement of expansive concrete and shrinking concrete beams just before loading and at the zero stress condition, and under load. The difference of strain change should result in an increase or decrease in crack width, a concept that has been incorporated into the equation for maximum crack width in the JSCE design code (JSCE 2002). The equation for maximum crack width in the same code is as follows:

$$w = 1.1k_1k_2k_3 \left\{ 4c + 0.7(c_s - \phi) \right\} \left[\frac{\sigma_{se}}{E_s} + \epsilon'_{csd} \right] \quad (4)$$

where, k_1 = a constant to take into account the effect of surface geometry of reinforcement on crack width, k_2 = a constant to take into account the effect of concrete quality on crack width given by $k_2 = 15(f'_c + 20) + 0.7$, f'_c = compressive strength of concrete (N/mm²), k_3 = a constant to take into account the effect of multiple layers of tensile reinforcement on crack width, n = number of layers of tensile reinforcement, c = concrete cover (mm), c_s = center-to-center distance of tensile reinforcement (mm), ϕ = diameter of tensile reinforcement (mm), σ_{se} = increment of stress of reinforcement from the state in which concrete stress at the

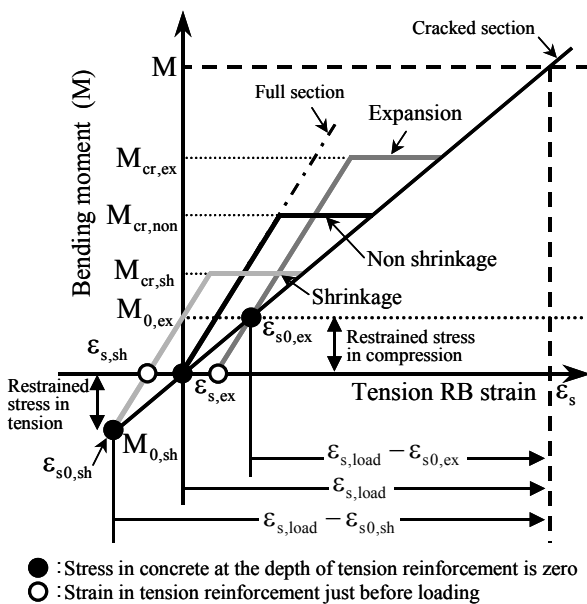


Fig. 10 Concept of effect of shrinkage/expansion on strain change in tension reinforcement.

portion of reinforcement is zero (zero stress condition) (N/mm²), and ϵ'_{csd} = compressive strain for evaluation of increment of crack width due to shrinkage and creep of concrete. ϵ'_{csd} of 100×10^{-6} is recommended for high-strength concrete.

Figure 11 shows the relationship between maximum crack width and stress change in tension reinforcement calculated by considering the aforementioned zero stress condition. The figure shows that there is little difference in the results among the various mixtures. **Figure 12** shows the relationship between maximum crack width and reinforcement strain at zero stress condition in order to make the effect of reinforcement strain accumulated before loading on crack width clear. The load-induced stress in tension reinforcement is calculated in accordance with conventional RC theory and is 200 N/mm². According to **Fig. 12**, the measured values of maximum crack width change proportionally with the variation in accumulated reinforcement strain due to the shrinkage/expansion of concrete before loading. It is obvious that this tendency can be evaluated satisfactorily by considering the strain change in tension reinforcing bars from the zero stress condition. Thus, it is demonstrated that crack widths of RC beams made of HSC having shrinkage/expansion before loading can be evaluated with acceptable accuracy by applying the proposed concept.

5.2 Curvature

Figure 13 shows the relationship between bending moment and average curvature. The average curvatures at the full and cracked sections of the NC1-RC beam calculated in accordance with conventional RC theory are also illustrated in the same figure. **Figure 13** shows that there is a significant difference between measured and calculated average curvatures at the cracked section, while there is good agreement at the full section. In some beams, which have significantly higher shrink-

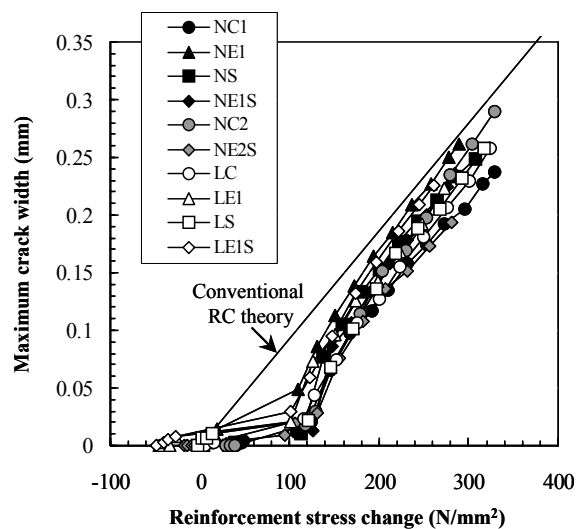


Fig. 11 Maximum crack width versus reinforcement stress change based on proposed concept.

age-induced stress, the measured average curvatures exceed the calculated ones, even though the tension-stiffening effect is involved in the measured average curvature. On the other hand, in the cases of beams that show expansion (LE1, LE1S), the calculated average curvatures significantly exceed the measured ones. This reason may be due to the fact that the shrinkage/expansion effect before loading is neglected in the calculations, even though the elastic strains created in concrete and reinforcements caused by shrinkage and expansion should influence the curvature.

Figure 14 demonstrates the strain distribution at the cross section before and after loading for both the shrinkage and expansion cases. The results show that shrinkage and expansion contribute to increasing and decreasing flexural deformation. Curvature induced by early age deformation ψ_{def} as well as curvature induced by early age deformation followed by loading ψ at a cracked section, are given by the following equations:

$$\begin{aligned} \psi &= \frac{\epsilon_{s,load} - \epsilon_{c,load}}{d} - \frac{\epsilon_{s,def} - \epsilon_{c,def}}{d} \\ &= \frac{\sigma_{s,load}/E_s - (\sigma_{c,load}/E_c + \epsilon_{c,free})}{d} \\ &\quad - \frac{\sigma_{s,def}/E_s - (\sigma_{c,def}/E_c + \epsilon_{c,free})}{d} \\ &= \frac{\sigma_{s,load}/E_s - \sigma_{c,load}/E_c}{d} - \frac{\sigma_{s,def}/E_s - \sigma_{c,def}/E_c}{d} \\ &= \psi_{load} - \psi_{def} \end{aligned} \tag{5}$$

where, $\sigma_{s,def}$ = shrinkage- or expansion-induced stress in tension reinforcement just before loading, $\sigma_{c,def}$ = shrinkage- or expansion-induced stress in concrete at the extreme upper fiber just before loading, and $\epsilon_{c,free}$ = free deformation at early ages. Based on Branson's equation (Branson 1963), effective flexural stiffness is

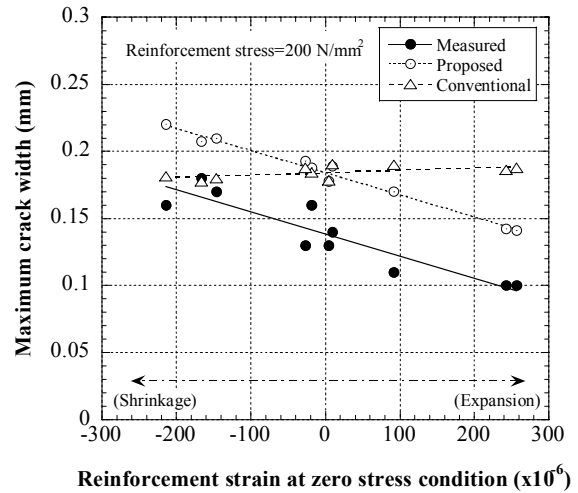


Fig. 12 Maximum crack width versus reinforcement strain at zero stress condition.

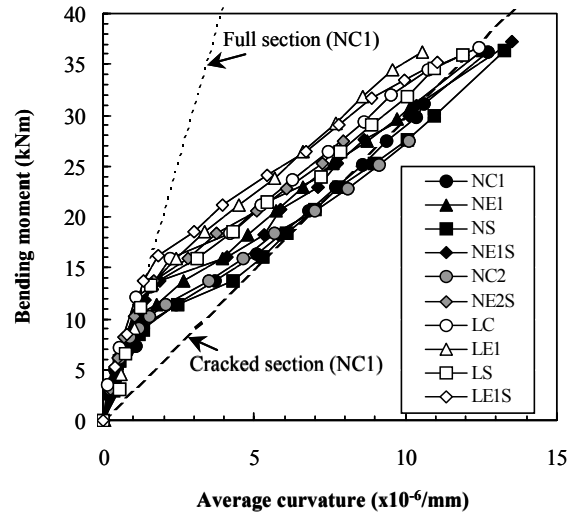


Fig. 13 Bending moment versus average curvature.

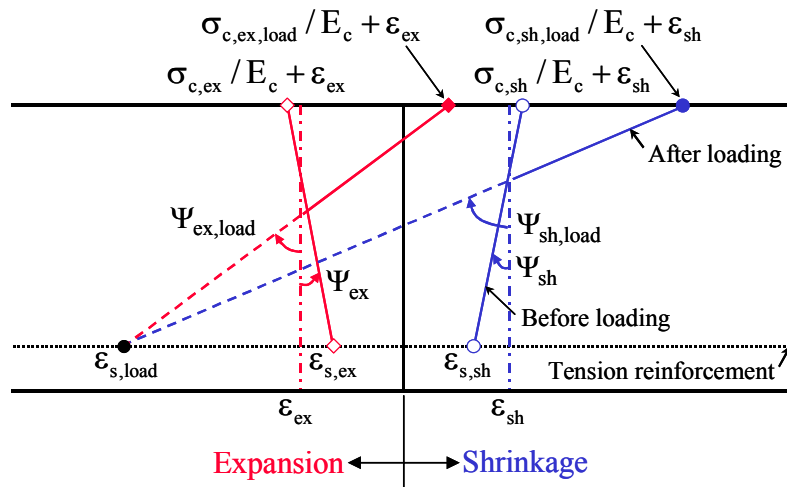


Fig. 14 Strain and stress distribution at cross section before and after loading.

modified by incorporating the shrinkage or expansion effect into flexural stiffness at cracked section as follows:

$$E_c I_c = \left(\frac{M_{cr}}{M_d}\right)^4 E_c I_g + \left(1 - \left(\frac{M_{cr}}{M_d}\right)^4\right) E_c I_{cr}$$

$$E_c I_{cr} = M_d / (\psi_{load} - \psi_{def}) \tag{6}$$

where, E_c = Young's modulus of concrete, I_g = moment of inertia of gross cross section, I_{cr} = moment of inertia of cracked cross section, M_{cr} = cracking moment, and M_d = applied moment.

The early age deformation effect-based moment-curvature relationship as well as the apparent moment-curvature relationship are schematically shown in **Fig. 15**, in which $M_{0,ex}$, $M_{0,sh}$ denote the moments of beams made of expansive concrete and shrinking concrete at the zero stress condition, ψ_{ex} , ψ_{sh} denote the curvatures of the same beams just before loading, and ψ_{load} denote the curvatures under load considered.

Figure 16 shows a typical example of the validity of the proposed concept for a moment-curvature relationship. The cracking moment of the proposed concept is calculated by using measured splitting tensile strength as well as concrete stress induced by early age deformation before loading. **Figure 17** shows the comparison between measured and calculated average curvature as a function of reinforcement strain at zero stress condition. The load-induced stress in tension reinforcement is calculated in accordance with conventional RC theory and is 200 N/mm². Comparisons between calculations and measurements indicate that the former predict the latter with satisfactory accuracy when considering early age deformation. However, the calculated value underestimates and overestimates the latter when the effects of

shrinkage and expansion, respectively, are neglected.

6. Conclusions

The importance of autogenous shrinkage to serviceability performance of reinforced high-strength concrete (HSC) flexural beams, and also the effectiveness of low-shrinkage HSCs (LS-HSC) that are made by using expansive additive and/or shrinkage-reducing chemical agent and/or Belite-rich low-heat Portland cement for improving the serviceability performance of beams, were investigated from the viewpoint of both experimental results and design equations. The following conclusions can be drawn from the present study.

- (1) Autogenous shrinkage of HSC significantly affects the increase in crack width and deformation of RC beams, while LS-HSCs markedly improve their serviceability performance.
- (2) The present concept taking into account strain change in tension reinforcement and curvature change at the cracked section before and after loading is effective in explaining the effects of shrinkage and expansion of concrete before loading on maximum crack width and flexural deformation under short-term loading.
- (3) JSCE code equations for predicting maximum crack width and flexural deformation into which the present concept is incorporated improve the prediction accuracy compared with conventional equations and show fairly good agreement with experimental results.

Acknowledgement

The authors express their sincere gratitude to the graduate and undergraduate students of Structural Materials Laboratories of Hiroshima University for performing numerous experiments.

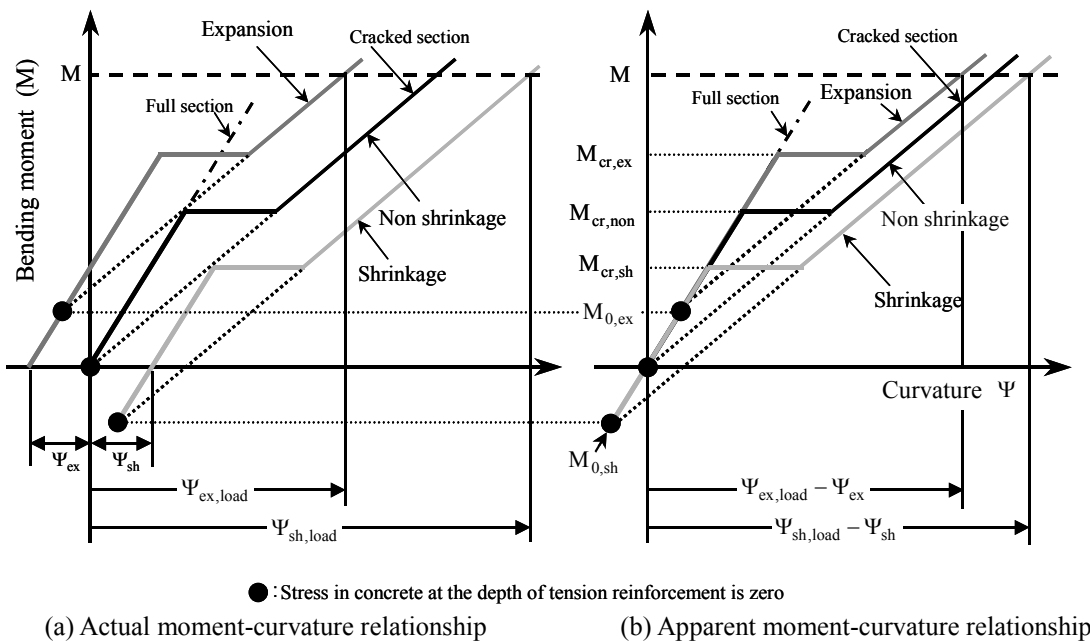


Fig. 15 Concept of effect of shrinkage/expansion on curvature of beam.

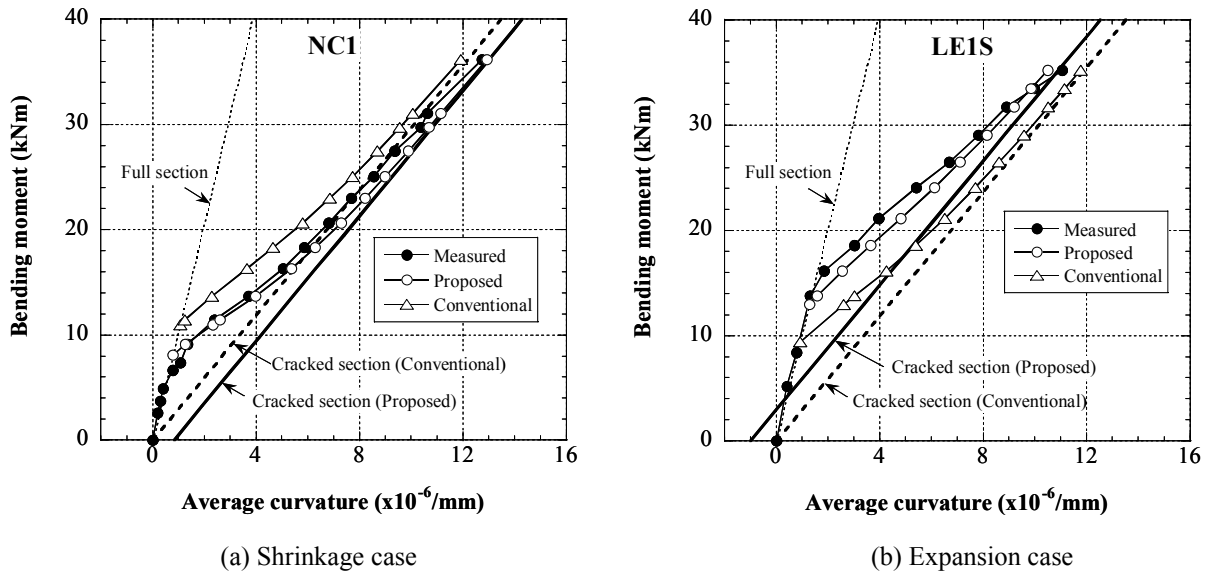


Fig. 16 Comparison between measured and calculated average curvature.

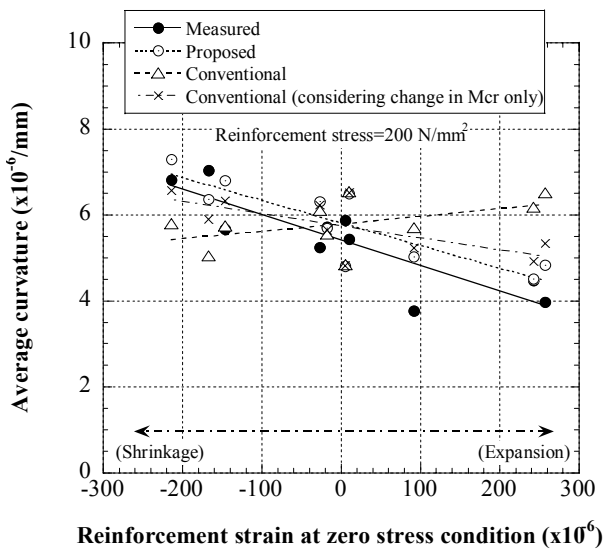


Fig. 17 Average curvature versus reinforcement strain at zero stress condition.

References

Bentur, A., Igarashi, S. and Kovler, K. (2001). "Prevention of autogenous shrinkage in high strength concrete by internal curing using wet lightweight aggregates." *Cement and Concrete Research*, 31, 1587-1591.

Bentz, D. P., Geiker, M. R. and Hansen, K. K. (2001). "Shrinkage-reducing admixtures and early-age desiccation in cement paste and mortars." *Cement and Concrete Research*, 31, 1075-1085.

Berke, N. S. and Li, L. (2003). "Effectiveness of

shrinkage reducing admixtures in reducing total shrinkage." *Advanced in Cement and Concrete*, Copper Mountain, Colorado, USA, 101-109.

Branson, D. E. (1963). "Instantaneous and time-dependent deflections of simple and continuous reinforced concrete beams." *HPR Report*, 7(1).

CEB, (1990). "CEB-FIP model code 1990." Thomas Telford, 61-62.

Chikamatsu, R., Takeda, N., Miura, N. and Sogo, S. (1997). "Study on lower shrinkage of high strength, high fluidity concrete." *Proceedings of the Japan Concrete Institute*, 19(1), 169-174. (in Japanese)

Holt, E. E. and Leivo, M. T. (2000). "Methods of reducing early-age shrinkage." *Proceedings of the International RILEM Workshop on Shrinkage of Concrete*, Shrinkage 2000, Paris, France.

Hori, A., Morioka, M., Sakai, E. and Daimon, M. (1998). "Influence of expansive additives on autogenous shrinkage." *International Workshop on Autogenous Shrinkage of Concrete*, JCI, Edited by E. Tazawa, Hiroshima, Japan, E & FN SPON, 187-194.

Hori, A., Andou, T., Otabe, Y. and Suzuki, Y. (2001). "Development of initial defect-free high-performance concrete." *Concrete Journal*, JCI, 39(8), 16-21. (in Japanese)

JCI, (1999). "Autogenous shrinkage of concrete" in: E. Tazawa, Ed. London: E & FN SPON, 21-26.

Jensen, O. M. and Hansen, P. F. (2001). "Water-entrained cement-based materials: I. principle and theoretical background." *Cement and Concrete Research*, 31, 647-654.

Jensen, O. M. and Hansen, P. F. (2002). "Water-entrained cement-based materials: II. Implementation and experimental results." *Cement and Concrete Research*, 32, 973-978.

- JSCE, (2002). "Standard specifications for concrete structures-2002, Structural performance verification." Japan Society of Civil Engineers, 114-117, 123-129.
- Kameta, S., Sato, R. and Abe, Y. (2000). "Stresses at joint interface between existing continuously reinforced concrete pavement and overlay concrete with expansive additive and shrinkage reducing agent." *4th International Workshop on Design Theories and Their Verification of Concrete Slabs for Pavements and Rail Roads*, 305-320.
- Miyazawa, S. and Tazawa, E. (1996). "Influence of cement composition on autogenous shrinkage of cementitious materials." *Proceedings of the Japan Concrete Institute*, 18(1), 699-704. (in Japanese)
- Ogawa, A., Sakata, K. and Tanaka, S. (1995). "A study on reducing shrinkage of highly-flowable concrete." *Second CANMET/ACI International Symposium on Advanced in Concrete Technology*, Las Vegas, Nevada, USA, 55-72.
- Paillere, A. M., Buil, M. and Serrano, J. J. (1989). "Effect of fiber addition on the autogenous shrinkage of silica fume concrete." *ACI Materials Journal*, 86(2), 139-144.
- Sato, R., Tanaka, S., Hayakawa, T. and Tanimura, M. (1999). "Experimental studies on reduction of autogenous shrinkage and its induced stress in high strength concrete." *Proceedings of the 2nd International Research Seminar on Self-Desiccation and Its Importance in Concrete Technology*, Lund, Sweden, 163-171.
- Sato, R., Masaki, S., Hiramatsu, Y. and Kodama, K. (2003). "Serviceability performance evaluation of reinforced high strength concrete beams." *2nd International Specialty Conference on the Conceptual Approach to Structural Design*, CI-Premier, Italy, 763-770.
- Schrage, I., Mangold, M. and Sticha, J. (1992). "An approach to high-performance concrete in Germany." *Fourth CANMET/ACI International Conference on Fly Ash, Silica Fume, Slag, and Natural Pozzolans in Concrete*, Istanbul, Turkey, Supplementary Papers, 493-511.
- Schwartzentruber, A., Philippe, M., Marchese, G. and Laurence, O. (2002). "Cracking tendency of UHSC-influence of fibers and expansive admixtures." *6th International Symposium on Utilization of High-Strength/High-Performance Concrete*, Vol. 2, Leipzig, Germany, 1391-1405.
- Takeuchi, M., Tanaka, S., Sato, R. and Ohno, Y. (1997). "Evaluation of the autogenous shrinkage of high strength concrete." *Proceedings of the Japan Concrete Institute*, 19(1), 751-756. (in Japanese)
- Tanimura, M., Hyodo, H., Sato, T. and Sato, R. (2000). "An investigation on reducing shrinkage of high strength concrete." *Proceedings of the Japan Concrete Institute*, 22(2), 991-996. (in Japanese)
- Tanimura, M., Hyodo, H., Omori, H. and Sato, R. (2001a). "Experimental study on reduction of shrinkage stress of high strength concrete." *Proceedings of the Japan Concrete Institute*, 23(2), 1075-1080. (in Japanese)
- Tanimura, M., Sato, R., Shimoyama, Y. and Omori, H. (2001b). "Improvement of flexural behavior of reinforced high strength concrete members by reducing autogenous shrinkage." *Concrete Science and Engineering*, 3 (11), 179-184.
- Tanimura, M., Hyodo, H., Nakamura, H. and Sato, R., (2002a). "Effectiveness of expansive additive on reduction of autogenous shrinkage stress in high-strength concrete." *Proceedings of the Third International Research Seminar on Self-Desiccation and Its Importance in Concrete Technology*, Lund, Sweden, 205-216.
- Tanimura, M., Hiramatsu, Y., Hyodo, H. and Sato, R. (2002b). "Flexural performance of RC members made of low shrinkage-high strength concrete." *6th International Symposium on Utilization of High-Strength/High-Performance Concrete*, Vol. 2, Leipzig, Germany, 1437-1452.
- Tazawa, E. and Miyazawa, S. (1992a). "Autogenous shrinkage of cement paste with condensed silica fume." *Fourth CANMET/ACI International Conference on Fly Ash, Silica Fume, Slag, and Natural Pozzolans in Concrete*, Istanbul, Turkey, Supplementary Papers, 875-894.
- Tazawa, E. and Miyazawa, S. (1992b). "Autogenous shrinkage caused by self desiccation in cementitious material." *9th International Congress on the Chemistry of Cement*, Vol. 4, New Delhi, India, 712-718.
- Tazawa, E., Miyazawa, S. and Sato, T. (1993). "Influence of cement composition on autogenous shrinkage." *JCA Proceedings of Cement & Concrete*, 47, 528-533. (in Japanese)
- Tazawa, E., Matsuoka, S., Miyazawa, S. and Okamoto, S. (1994). "Effect of autogenous shrinkage on self stress in hardening concrete." *International RILEM Symposium on Thermal Cracking in Concrete at Early Ages*, 221-228.
- Tazawa, E. and Miyazawa, S. (1995). "Influence of cement and admixture on autogenous shrinkage of cement paste." *Cement and Concrete Research*, 25, 281-287.
- Tazawa, E. and (1997). "Influence of constituents and composition on autogenous shrinkage of cementitious materials." *Magazine of Concrete Research*, 49(178), 15-22.
- Weiss, W. J., Borichevsky, B. B. and Shah, S. P. (1999). "The influence of a shrinkage reducing admixture on early-age shrinkage behavior of high performance concrete." *5th International Symposium on Utilization of High Strength/High Performance Concrete*, 2, Sandefjord, Norway, 1339-135